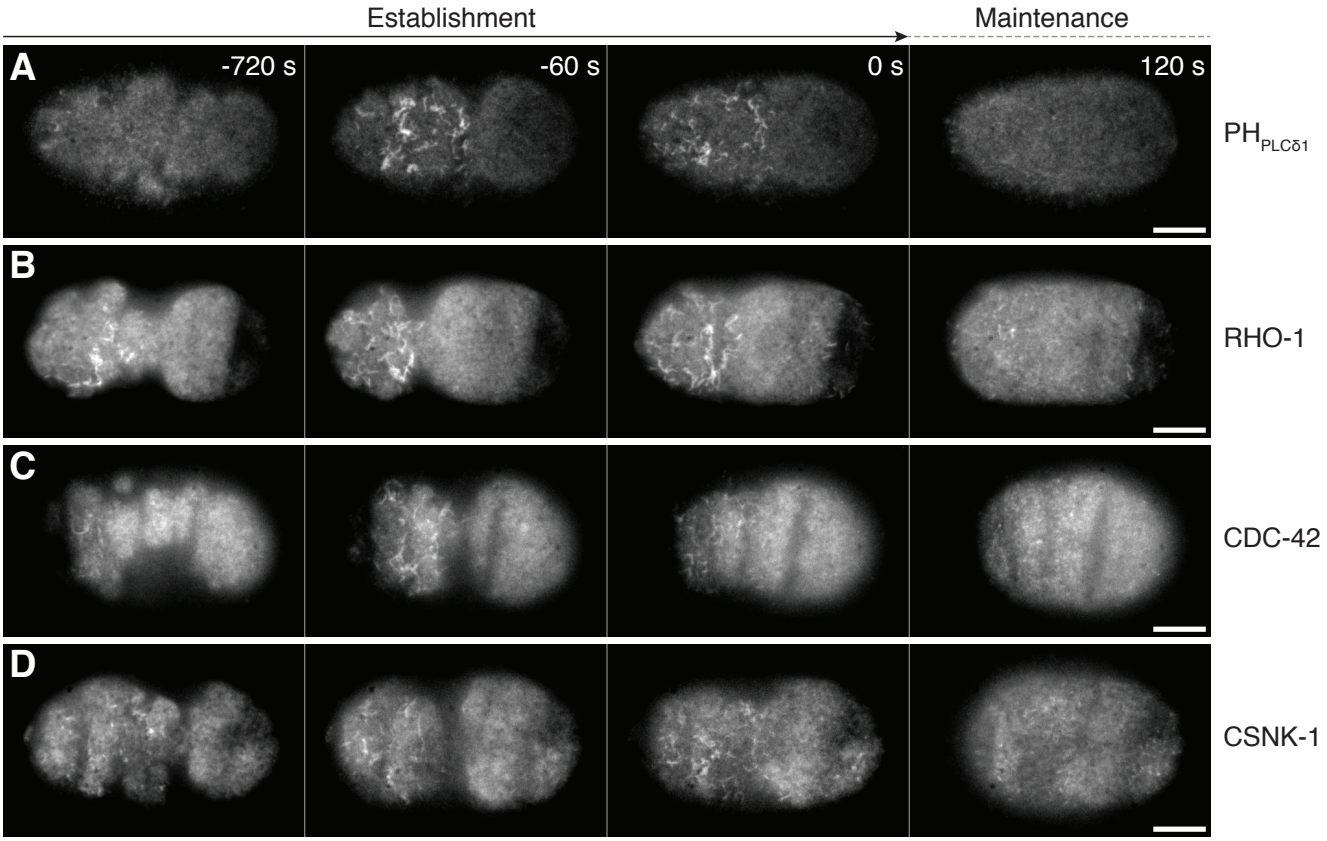

Figure S1. Diverse signaling molecules appear enriched in cortical structures. (A-D) HiLo microscopy images of mCherry::$PH_{PLC\delta1}$ (n>5) (A), GFP::RHO-1 (n = 2) (B), CDC-42::mCherry (n = 3) (C), and GFP::CSNK-1 (n = 2) (D) at the cell cortex are shown from early symmetry-breaking to maintenance phase. All show cortical structures with a distinct pattern of appearance, subsequent enrichment in the anterior and dissipation upon entry to maintenance phase. Time (s) relative to the end of establishment phase. Scale bar = 10 um.

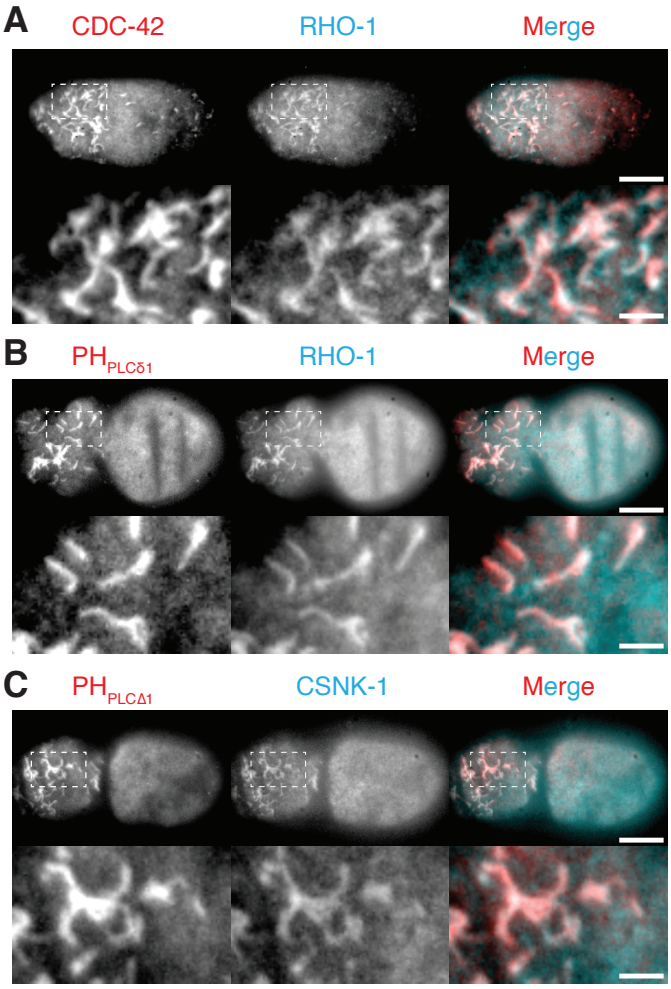

Figure S2. Colocalization of signaling molecules with the PIP_2 probe $PH_{PLC\delta1}$. (A) Sample image of surface of embryo co-expressing GFP::RHO-1 and mCherry CDC-42. Individual channels and merge shown with zoom of inset region to highlight structures. **(B)** As in (A), but GFP::RHO-1 with mCherry::$PH_{PLC\delta1}$. **(C)** As in (A), but GFP::CSNK-1 with mCherry::$PH_{PLC\delta1}$. Co-enrichment quantified in Figure 1B. Scale bars = 10 um.

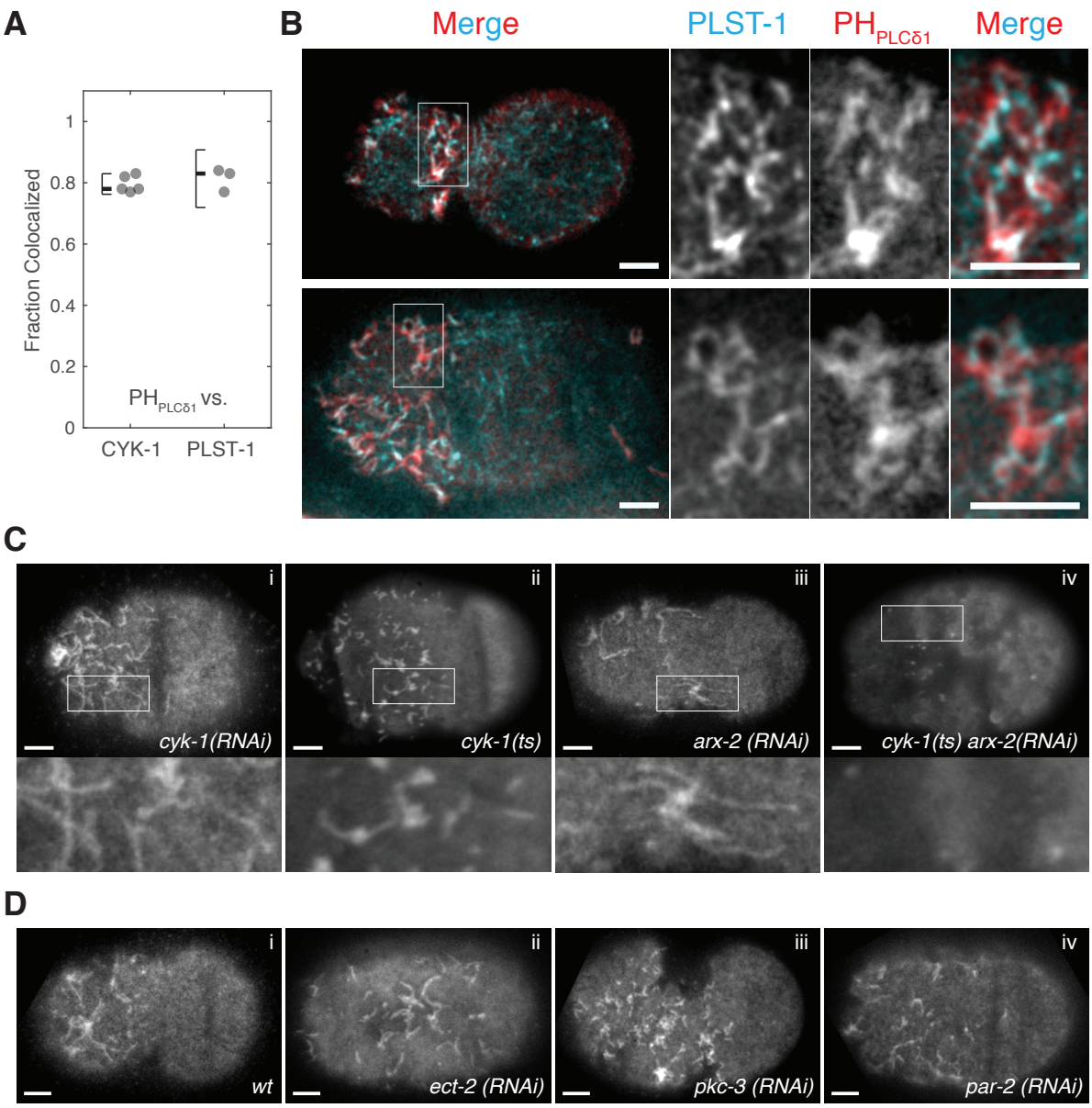

Figure S3. Filopodia are enriched in actin bundling proteins, require actin polymerization, and respond to polarity cues. (A) Fraction of selected $PH_{PLC\delta1}$-labeled structures that exhibit colocalized CYK-1 puncta at tips or enrichment in PLST-1. Datapoints from individual embryos shown. Median ± 95%CI indicated. **(B)** Cortical images of two embryos expressing PLST-1::GFP and mCherry::$PH_{PLC\delta1}$. Inset is marked and magnified on right showing merged and single channel images. **(C)** Disruption of both CYK-1 and ARX-2 lead to loss of filopodia like structures. mCherry (i,iii) or GFP (ii,iv) fusions to $PH_{PLC\delta1}$ persist when either ARX-2 or CYK-1 are disrupted on their own, but not when both are compromised. Insets magnified below to highlight filopodia structure. **(D)** Formation of filopodia is not affected when contractility is compromised by depletion of the RhoGEF, ECT-2, or when polarity is disrupted by depletion of PKC-3 or PAR-2 by RNAi. However, asymmetry of filopodia is reduced in all three cases consistent with their asymmetry requiring polarity. ECT-2 depletion compromises symmetry-breaking during the establishment phase (***Zonies et al., 2010***). Images shown reflect a timepoint of peak filopodial density just before relaxation of the cortex and filopodial disassembly. Scale bars = 5 μm.

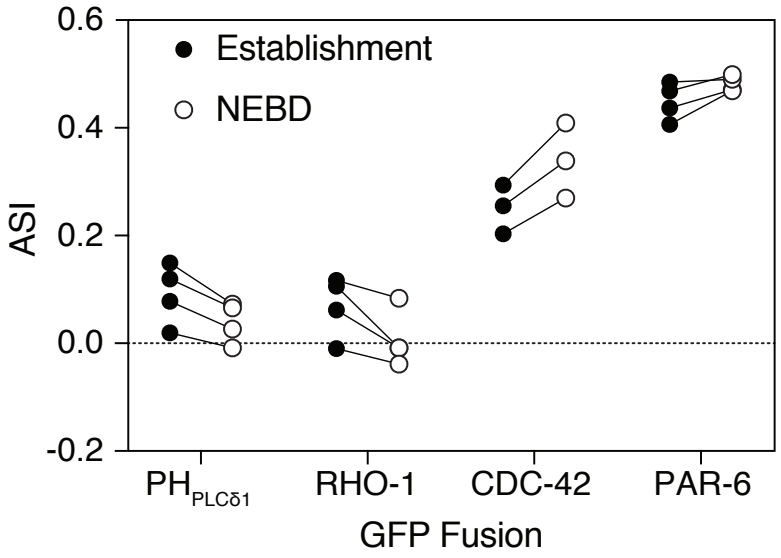

Figure S4. Asymmetry in membrane concentration from midplane images. Membrane fluorescence profiles were traced from midplane images of embryos expressing the indicated GFP fusions at mid-establishment (5 min pre-NEBD) or mid-maintenance phase (NEBD). For each embryo the asymmetry index (ASI) was calculated at each timepoint from the extracted profiles. Note asymmetry of both $PH_{PLC\delta1}$ and RHO-1 is low at establishment phase and is reduced further at maintenance phase when filopodia dissipate, consistent with filopodia contributing to weak apparent asymmetry during the establishment phase. By contrast, CDC-42 exhibits moderate asymmetry during establishment when anterior filopodia are high, but its asymmetry increases further by NEBD, when filopodia dissipate. For reference, the polarity protein PAR-6, which is not prominently enriched in these structures due to association with PAR-3 clusters, is highly polarized at both time points. Together these data suggest that filopodia-like structures, despite being highly asymmetric, do not contribute significantly to overall polarity in membrane concentrations.

Table S1. *C. elegans* strains used in this work.

Strain	Genotype	Source
ACR004	*cyk-1(ges1[cyk-1::eGFP + LoxP unc-119(+) LoxP] III; unc-119 (ed3) III; ltIs44pAA173; [pie-1p::mCherry::PH(PLC1delta1) + unc-119(+)] V*	This work
ACR010	*plst-1(ges2[plst-1::eGFP + LoxP unc-119(+) LoxP] IV; unc-119 (ed3) III; ltIs44pAA173; [pie-1p::mCherry::PH(PLCδ1) + unc-119(+)] V*	This work
AD189	*unc-119(ed3) III; asIs2[unc-119(+) + pie-1p::GFP::egg-1]*	CGC, ***Kadandale et al.*** (***2005***)
FT204	*unc-119(ed3) III; xnIs87[syn-4p::GFP::syn-4::syn-4 3'UTR + unc-119(+)]*	CGC
JA1354	*unc-119(e2498) III; weIs12[unc-119(+) + pie-1p::GFP::csnk-1]*	CGC, ***Panbianco et al.*** (***2008***)
JCC146	*cyk-1(or596ts); unc-119(ed3); ltIs38 [pAA1; pie-1p::GFP::PH(PLCδ1) + unc-119 (+)]; ltIs37 [pAA64; pie-1p::mCherry::his-58; unc-119 (+)]IV*	***Jordan et al.*** (***2016***)
KK1248	*par-6(it310[par-6::gfp]) I*	CGC, Ken Kemphues
NWG0045	*unc-119(ed3) III; crkIs16[mex-5p::mKate::iLiD::nmy-2 3'UTR + unc-119(+)]*	This work
NWG0047	*unc-119(ed3)III; crkEx1[pNG19: mex-5p::PH(PLCδ1)::GBP::mKate::nmy- 2 3'UTR + unc-119(+)]; him-5 (e1490) V*	***Rodriguez et al.*** (***2017***)
OD58	*unc-119(ed3) III; ltIs38[pAA1; pie-1p::GFP::PH(PLCδ1) + unc-119(+)]*	CGC, ***Audhya et al.*** (***2005***)
OD70	*unc-119(ed3) III; ltIs44pAA173; [pie-1p-mCherry::PH(PLCδ1) + unc-119(+)] V*	CGC, ***Kachur et al.*** (***2008***)
SA115	*tjIs1[pie-1::GFP::rho-1 + unc-119(+)]*	CGC, ***Motegi and Sugimoto*** (***2006***)
SWG1	*mex-5p::Lifeact::mKate2*	***Reymann et al.*** (***2016***)
SWG5	*plst-1(ges2[plst-1::eGFP + LoxP unc-119 (+) LoxP] IV; unc-119 (ed3) III)*	***Reymann et al.*** (***2016***)
SWG19	*cyk-1(ges1[cyk-1::eGFP + LoxP unc-119(+) LoxP) III; unc-119(ed3) III.*	***Reymann et al.*** (***2016***)
TH159	*ddIs46[WRM0625bA11 GLCherry::cdc-42; Cbr-unc-119(+)]*	***Rodriguez et al.*** (***2017***)
TH220	*unc-119(ed3) III; ddIs86[pie-1p::LifeAct::GFP; unc-119(+)]*	***Redemann et al.*** (***2010***)
WS5018	*cdc-42(gk388) opIs295[cdc-42p::GFP::cdc-42(genomic)::cdc-42 3'UTR + unc-119(+)] II.*	CGC, ***Neukomm et al.*** (***2014***)

Movie 1. Timelapse video of the surface of a permeabilized embryo expressing $PH_{PLC\delta1}$::GFP (middle, cyan) and stained with FM4-64 (left, red). Scale bar, 2.5 µm. Elapsed time (sec). See related Figure 1F.

Movie 2. Timelapse video of filopodia extending into the pseudocleavage furrow in an embryo expressing CYK-1::GFP and mKate$_{myr}$. Scale bar, 5 µm. Elapsed time (mm:ss) shown. See related Figure 2A.

Movie 3. Timelapse video of dynamic filopodia on the surface of an embryo expressing CYK-1::GFP and $_{PLC\delta1}$::mCherry. Scale bar, 5 µm. Elapsed time (sec) shown. See related Figure 2D.

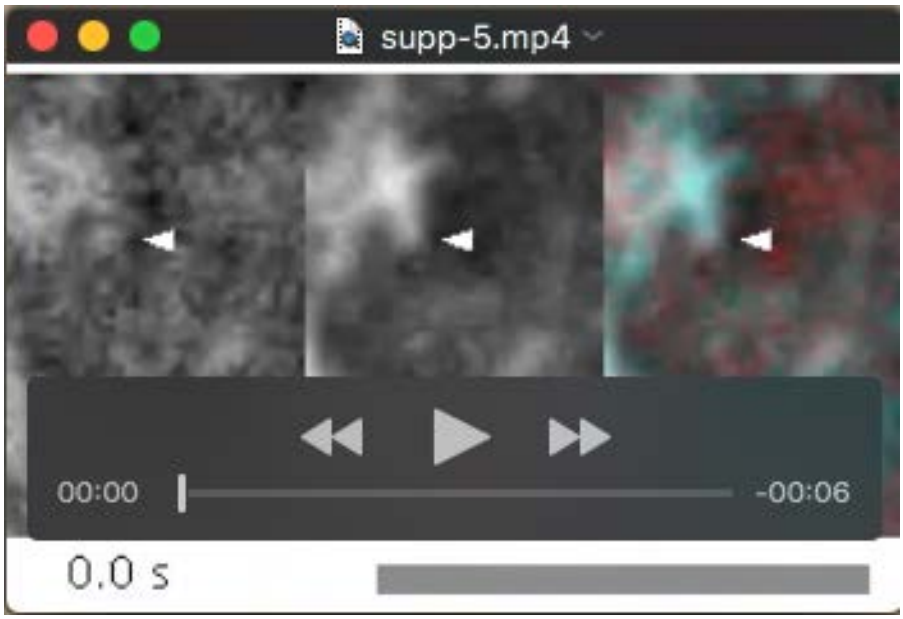

Movie 4. Timelapse video of an extending filopodium labeled with LifeAct::GFP and $_{PLC\delta1}$::mCherry on the surface of a one-cell embryo. Elapsed time (sec) shown. Scale bar, 5 µm. See related Figure 2F.

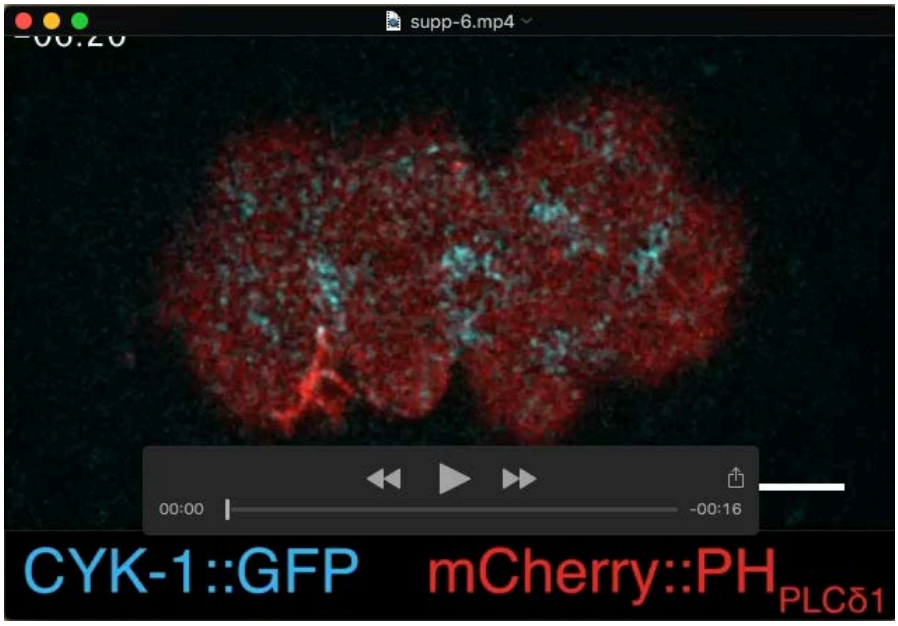

Movie 5. Timelapse video of the surface of an embryo expressing CYK-1::GFP and $PH_{PLC\delta1}$::mCherry by confocal microscopy showing the appearance, accumulation, segregation and dissipation of filopodia. Elapsed time shown (mm:ss). Scale bar, 5 µm. See related Figure 2K.

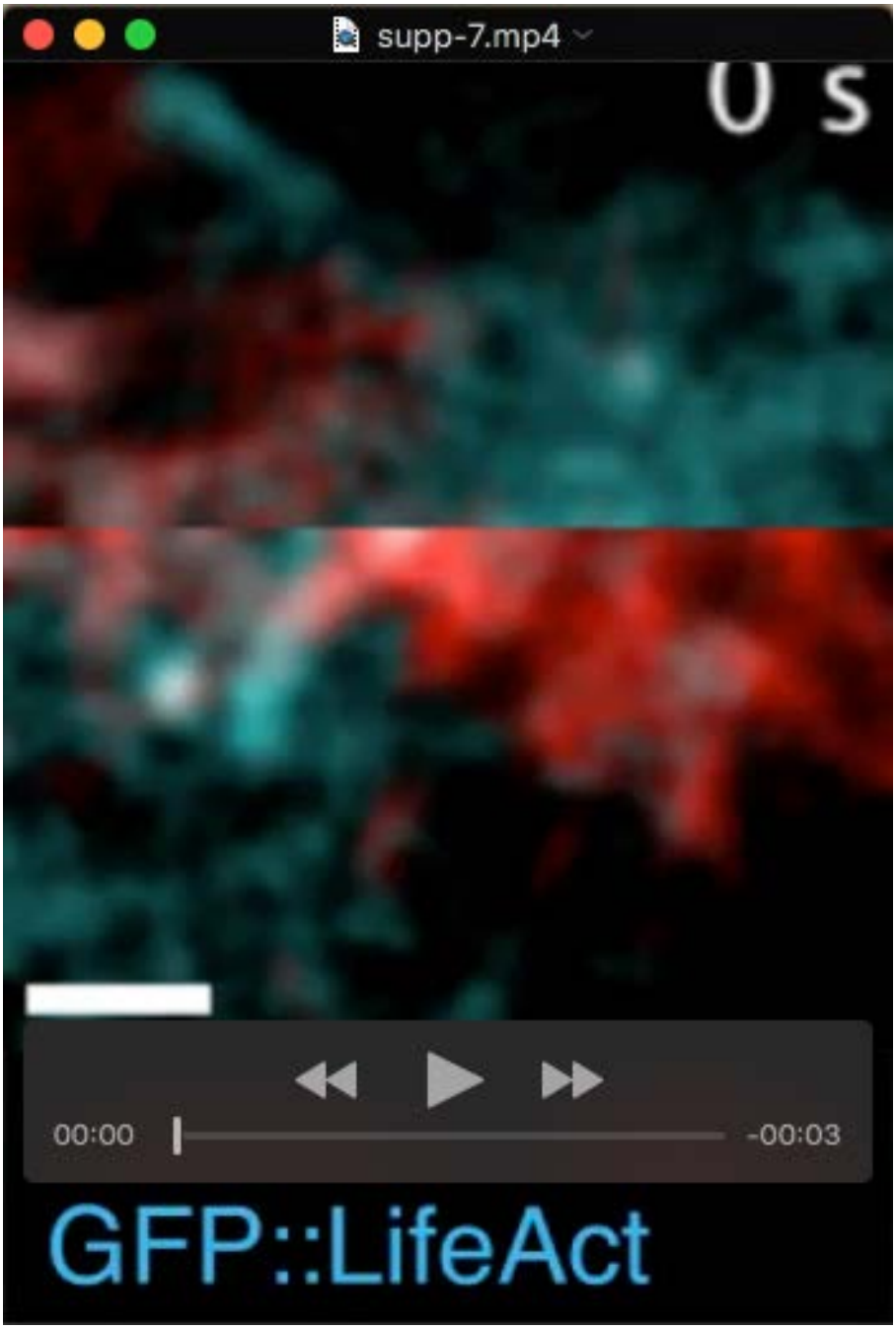

Movie 6. Timelapse video of two filopodia labeled with LifeAct::mKate (red) and LifeAct::GFP (cyan) corresponding to straightened filopodia shown in Figure 3E. Note lag of LifeAct::mKate signal relative to LifeAct::GFP yielding a cyan tip followed by a red tail. Elapsed time shown (sec). Scale bar, 2.5 µm. See related Figure 3F-G.

Journal of Cell Science • Supplementary information

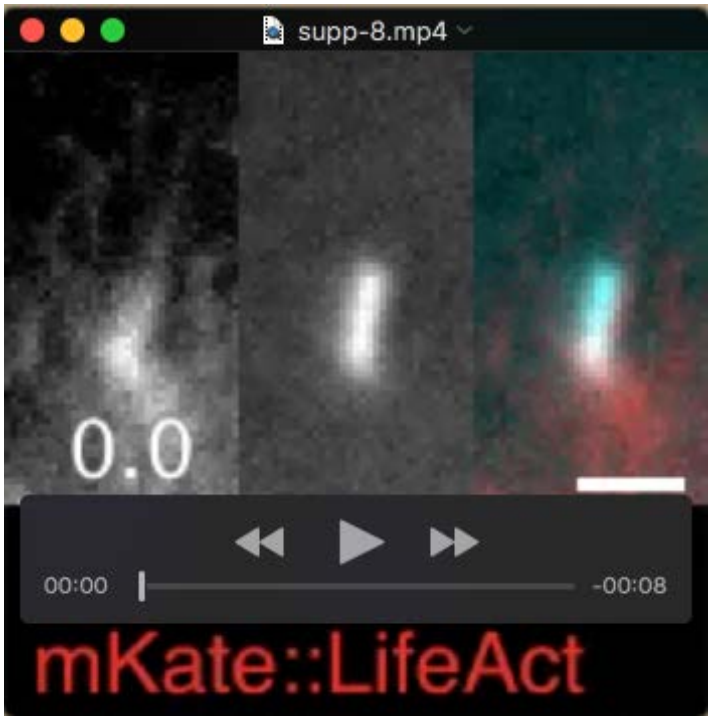

Movie 7. Timelapse video of cytoplasmic actin comet labeled with LifeAct::mKate (red) and LifeAct::GFP (cyan). Note lag of LifeAct::mKate signal relative to LifeAct::GFP yielding a cyan tip followed by a red tail. Elapsed time shown (sec). Scale bar, 2.5 μm. See related Figure 3G-H.

References

Audhya A., Hyndman F., McLeod I.X., Maddox A.S., Yates J.R., Desai A., Oegema K. (2005). A complex containing the Sm protein CAR-1 and the RNA helicase CGH-1 is required for embryonic cytokinesis in *Caenorhabditis elegans*. *J. Cell Biol.* 171, 267–279.

Cuenca A.A., Schetter A., Aceto D., Kemphues K., Seydoux G. (2003). Polarization of the *C. elegans* zygote proceeds via distinct establishment and maintenance phases. *Development* 130, 1255–1265.

Jordan S.N., Davies T., Zhuravlev Y., Dumont J., Shirasu-Hiza M., Canman J.C. (2016). Cortical PAR polarity proteins promote robust cytokinesis during asymmetric cell division. *J. Cell Biol.* 212, 39–49.

Kachur T.M., Audhya A., Pilgrim D.B. (2008). UNC-45 is required for NMY-2 contractile function in early embryonic polarity establishment and germline cellularization in *C. elegans*. *Dev. Biol.* 314, 287–299.

Neukomm L.J., Zeng S., Frei A.P., Huegli P.A., Hengartner M.O. (2014). Small GTPase CDC-42 promotes apoptotic cell corpse clearance in response to PAT-2 and CED-1 in *C. elegans*. *Cell Death Differ.* 21, 845–853.

Redemann S., Pecreaux J., Goehring N.W., Khairy K., Stelzer E.H.K., Hyman A.A., Howard J. (2010). Membrane Invaginations Reveal Cortical Sites that Pull on Mitotic Spindles in One-Cell *C. elegans* Embryos. *PLoS ONE.* 5, e12301.

Zonies S., Motegi F., Hao Y., Seydoux G. (2010). Symmetry breaking and polarization of the *C. elegans* zygote by the polarity protein PAR-2. *Development* 137, 1669–1677.